Journal of Cleaner Production 340 (2022) 130752

Contents lists available at ScienceDirect

Journal of Cleaner Production

journal homepage: www.elsevier.com/locate/jclepro

Assessment of the potential of floating solar photovoltaic panels in bodies of water in mainland Spain

M. López [a,*], F. Soto [a], Z.A. Hernández [b]

[a] DyMAST Research Group & Dept. of Construction and Manufacturing Engineering, Universidad de Oviedo, Escuela Politécnica de Mieres C/ Gonzalo Gutiérrez Quirós s/n, 33600, Mieres, Asturias, Spain

[b] GICONSIME Research Group & Dept. of Construction and Manufacturing Engineering, Universidad de Oviedo, Escuela Politécnica de Mieres C/ Gonzalo Gutiérrez Quirós s/n, 33600, Mieres, Asturias, Spain

ARTICLE INFO

Handling Editor: Zhen Leng

Keywords:
Renewable energy
Solar energy
Floatovoltaics
Floating structures
LCOE

ABSTRACT

This article presents the potential of floating photovoltaic solar energy in Spain, a country with a high solar energy resource and a large water surface area for its deployment, for the first time. Geodata for natural, artificial, and highly modified bodies of freshwater, along with environmental geospatial datasets, were used to calculate electricity generation, taking into account the positive water-cooling effect. The results revealed that Spain could meet about 31% of its electricity demand by covering only 10% of the available water surface area. Deployment of the country's full floating photovoltaic potential could reduce non-renewable electricity generation by 81% and greenhouse gas emissions by 6%, thereby helping to meet the European Union 2030 target. Spanish regions could benefit from this renewable energy, not only by reducing their dependence on non-renewable resources, but also by balancing their electricity generation and demand. The potential of this renewable energy technology is higher in southern regions and particularly in Extremadura, where the electricity generation potential is three times the electricity demand. A detailed analysis of the floating photovoltaic potential in three dam reservoirs, the Borbollón, La Pedrera and Guadalcacín, is also presented for four coverage scenarios. The results highlight the importance of including water depth restrictions on floating photovoltaic module operation and variations in reservoir water level in future assessments, rather than simply applying a fixed percentage of coverage.

1. Introduction

The scarcity of habitable land, growing energy consumption and environmental concerns about fossil fuels are fostering development of renewable energy technologies. In keeping with this trend, the European Union (EU) goal is to become a climate neutral country by 2050, setting intermediate targets for 2030 that include at least 55% cuts in greenhouse gas emissions (GHG) from 1990 levels. Spain, as a UE member state, is still far from this target and has lowered its emissions by only 10%, from 288.4 10^6 to 259.3 10^6 tCO_2 equivalent in 2019. Therefore, the non-renewable electricity generation of the country, 38.9% of the 2019 total, must be drastically reduced (REE, 2021).

Solar energy has experienced remarkable growth during the last decade due to the reduction in photovoltaic (PV) module manufacturing costs (Feldman et al., 2015). Apart from the traditional ground-mounted and rooftop PV modules, an emerging application, called floating PV (FPV) systems, sites PV modules directly on water (Fig. 1) (El Hammoumi et al., 2021). Although several commercial designs are available, FPV systems generally consist of conventional solar modules mounted on floaters, which provide buoyancy to the whole arrangement while anchored to the bottom of the water body (Oliveira-Pinto and Stokkermans, 2020). These systems withstand fluctuating water levels, however, they are not commonly designed to operate while resting on the bottom if the body of water is drained (Spencer et al., 2019). Like ground-mounted PV modules, FPV modules may be flat, tracking or tilted, commonly at an 11° angle (Redón Santafé et al., 2014).

The main advantage of FPV lies in the cooling effect of the water on the solar cells, which promotes higher energy conversion efficiency (Skoplaki and Palyvos, 2009). In fact, solar panels on water can generate up to 10% more electricity than on land (Kamuyu et al., 2018). Other advantages of this renewable energy technology include the availability of abundant water for cleaning the modules, system scalability from

* Corresponding author.
E-mail address: mario.lopez@uniovi.es (M. López).

https://doi.org/10.1016/j.jclepro.2022.130752
Received 17 May 2021; Received in revised form 3 January 2022; Accepted 28 January 2022
Available online 3 February 2022

microwatt to megawatt, reduction in growth of algae from shading by the modules, and the reduction of natural evaporation in water reservoirs (Santafé et al., 2014).

On another note, synergies could be developed in combination with many other activities. For example, generation by pumped-storage power systems could benefit considerably from integrated FPV modules which would also minimize the energy imbalance (Liu et al., 2019). Pringle et al. (2017) suggested the dual use of water areas for floating solar energy and aquaculture installations as an efficient use of water for both food and energy generation. The combination of FPV and solar water heating systems at various scales has also been proposed for mining applications (Taboada et al., 2017). Furthermore, the use of FPV power plant pontoons for compressed air energy storage was presented by Cazzaniga et al. (2017). Combination of FPV with other renewable energy sources such as wind (López et al., 2020) and wave energy (Oliveira-Pinto et al., 2020), has been demonstrated to improve power systems by smoothing power output.

Although the Levelized Cost of Energy (LCOE) is still higher than for ground-mounted PV solar plants (96.2–50.3 vs 35–40 €/MWh, respectively, Oliveira-Pinto and Stokkermans (2020), an increase in capacity could drastically reduce the cost of energy of floating FPV systems (Gorjian et al., 2021). Moreover, the installation of commercial FPV power plants is rapidly increasing in freshwater bodies such as lakes, and irrigation and dam reservoirs (Ranjbaran et al., 2019), and could also be deployed in pit lakes of abandoned and remote mines (Song and Choi, 2016). Within the many possibilities for FPV plant installation, man-made bodies of freshwater have been reported to be more suitable than natural, which is just as well, as their environmental impact on natural basins is still to be determined (Pimentel Da Silva and Branco, 2018). Offshore installation is still limited due to the harsh environmental loads and saltwater corrosion, but some novel concepts are also under development for this environment (Trapani and Millar, 2014).

Some authors have suggested that about 25% of the world's electricity demand could be supplied by covering just 1% of man-made bodies of water with FPV systems (Tina et al., 2018). However, detailed assessments of this resource are scarce and only a few studies have analysed its potential on a national or regional scale. Spencer et al. (2019) assessed the potential of FPV systems on artificial bodies of water at least 2 m deep in the continental United States, and concluded that 9.6% of the country's electricity generation could potentially be generated by covering 27% of the available surface of those water bodies with FPV. Zubair et al. (2020) showed that FPV covering 28% of the surface of one of Pakistan's main reservoirs would be enough to meet the country's electricity power shortage. Potential FPV production in South Korean reservoirs was estimated by Kim et al. (2019), assuming solar panels installed on 10% of the surface of reservoirs with an average water depth of 5 m. The performance of FPV systems in weirs of the Brazilian semiarid region was analysed by Padilha Campos Lopes et al. (2020) under three different scenarios of the surface cover and, more recently, the FPV potential in African hydropower reservoirs was evaluated for different reservoir coverage areas (Gonzalez Sanchez et al., 2021).

A fixed percentage of coverage is commonly applied in previous assessments to define the useful water surface for FPV module deployment, which is a parameter of paramount importance for accurate estimation of the power potential. However, the useful water surface depends on the minimum water depth for the operation of the FPV systems and the temporary oscillations in the water level (Kim et al., 2019). Moreover, previous assessments fail to consider the water-cooling effect, which is one of the main advantages of deploying PV modules in bodies of water.

Renewable energy resources are Spain's main energy asset for reducing GHG emissions, and solar energy has the highest potential (Girard et al., 2016). Previous analyses have already found the potential of ground-mounted PV (Martín-Martínez et al., 2019) and rooftop-mounted PV in this country (Gomez-Exposito et al., 2020). Moreover, a hybrid pump-as-turbine/solar pilot system for the agricultural sector was proposed in Merida García et al. (2021). However, the potential of FPV energy in Spain remains unexplored, even though the country has a vast freshwater surface area spread over more than 700 bodies of continental water (MITECO, 2019). The first FPV solar plant of this country was installed very recently and therefore data on the actual electricity generation potential is unavailable, which makes estimates even more necessary to plan future plants.

This study assessed the national and regional potential of FPV electricity generation in Spain using a geospatial database of both artificial and natural bodies of water and numerical meteorological databases for continental Spain. A first general assessment assumed FPV modules with a horizontal tilt angle and a fixed percentage of water surface coverage. Then, four different coverage scenarios and various tilt angles were analysed in detail for three specific dam reservoirs. The potential of these reservoirs is discussed in terms of the capacity factor (*CF*), the specific energy yield (*SE*) and the Levelized Cost of Energy (*LCOE*). As a novelty, the variations in the water level over time and FPV operation depth restrictions were included in some scenarios to reduce uncertainty in reservoir coverage. In addition, the calculations of the electricity generation account for the water-cooling effect on PV module power performance. The findings will help developers and promoters forecast

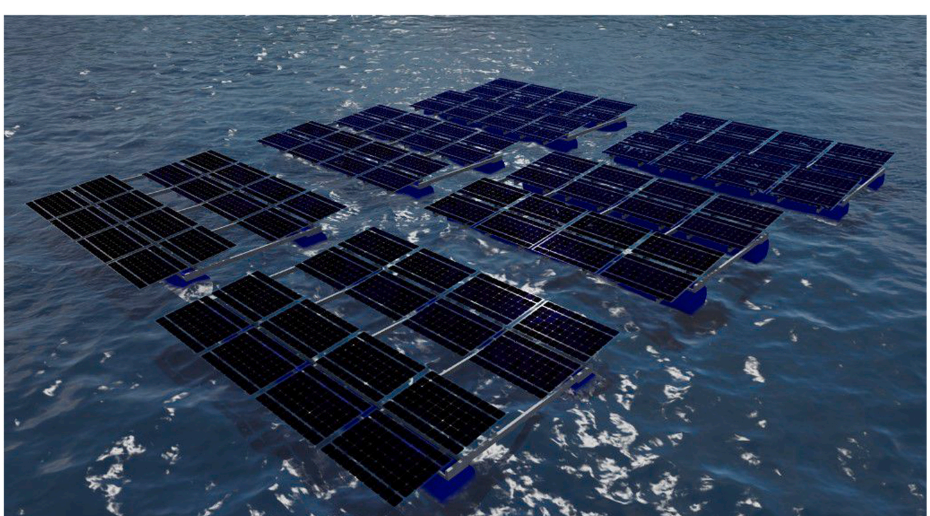

Fig. 1. Floating photovoltaic (FPV) system.

the electricity production of future FPV projects and select the best sites for installation of this promising technology.

The remainder of this paper is structured as follows. Section 2 presents the methodology and data, including a description of the bodies of water and regions of Spain, formulas for estimating FPV electricity generation and the geospatial datasets used. In Section 3, results are presented and discussed. Finally, conclusions are drawn in Section 5 and future lines of research are suggested.

2. Material and methods

2.1. Regions of peninsular Spain

Spain is divided into 17 peninsular and insular (Canary Islands and Balearic Islands) administrative regions. As neither of the two insular regions have significant freshwater bodies, they were excluded from this analysis. This study was therefore restricted to the 15 peninsular regions of Spain, which span an area of nearly 500,000 km^2 between latitudes 43.82° and 36.01°, and longitudes −9.29° and 3.32° (Fig. 2 and Table 1).

The Spanish regions vary widely in area. For instance, the largest region, Andalusia, spans an area seventeen times the area of La Rioja, the smallest region (Table 1). Their electricity demand and generation balance also differ widely. For example, in 2019, although the electricity demand in Catalonia was ten times higher than in Cantabria with balanced generation, Cantabria generated only just over half of its electricity demand. In the same year, about 40% of electricity in Spain was generated from non-renewable energy with noticeable differences among the regions (REE, 2021). While Galicia generated 65.2% of its electricity from non-renewable sources, only 13.6% was from non-renewables in the Basque Country.

2.2. Water bodies in peninsular Spain

Data on water bodies were retrieved from the Spanish Ministry for Ecological Transition and Demographic Challenge (MITECO) (MITECO, 2019). This dataset defines a surface body of water as "a significant discrete element of surface water such as a lake, a reservoir, a stream, river or canal, part of a stream, river or canal, transitional water or a stretch of coastal water" (European Comission, 2000). In the scope of this study, only inland standing bodies of water were analysed, as offshore FPV technology applications are still in a conceptual stage (Trapani and Millar, 2013). The bodies of water in the dataset are classified as highly modified water bodies, artificial water bodies and natural water bodies.

Artificial and modified bodies of water may be more suitable for FPV development than natural bodies of water (Spencer et al., 2019). Nonetheless, although FPV in natural bodies of water may cause a more substantial impact than on artificial water bodies, further research is required to assess the magnitude of this impact, and so they were also included here (Pimentel Da Silva and Branco, 2018).

According to MITECO, there are 745 inland water bodies in peninsular Spain, which is a total water surface area of 4194 km^2 (Fig. 3). This is a conservative figure, however, since FPV systems could be deployed on small water bodies that are not included in the MITECO dataset, this could result in an underestimation of the true potential. Of the total, 427 are artificial or highly modified water bodies (mainly corresponding to dammed water bodies) that come to a total water surface area of 3074 km^2.

Andalusia is the Spanish region with the most surface bodies of water with 152, followed by Catalonia and Castile-La Mancha with 112 and 108, respectively. In terms of total water surface area, Andalusia, with 1711 km^2, again has the largest inland water surface, followed by Castile-La Mancha and Extremadura, both with about 400 km^2. As shown in Fig. 3, the northern regions have fewer bodies of water and, in general, less water surface area than in the south.

The regions can also be compared in terms of the density of water bodies, which is found by dividing the water surface area by the total land area (Kim et al., 2019). The highest density corresponds to Extremadura (2.20%), followed by Andalusia (1.78%). On the contrary, the lowest densities are found in the smaller northern regions (e.g., Asturias, Cantabria, and Navarre's densities are below 0.20%) and Murcia (0.11%).

2.3. Selection of water bodies and FPV coverage scenarios

Since man-made bodies of water could be more suitable for this renewable energy technology, FPV electricity generation and economic potential were analysed for three dam reservoirs in different regions of Spain, the Guadalcacín (Andalusia), La Pedrera (Valencia) and

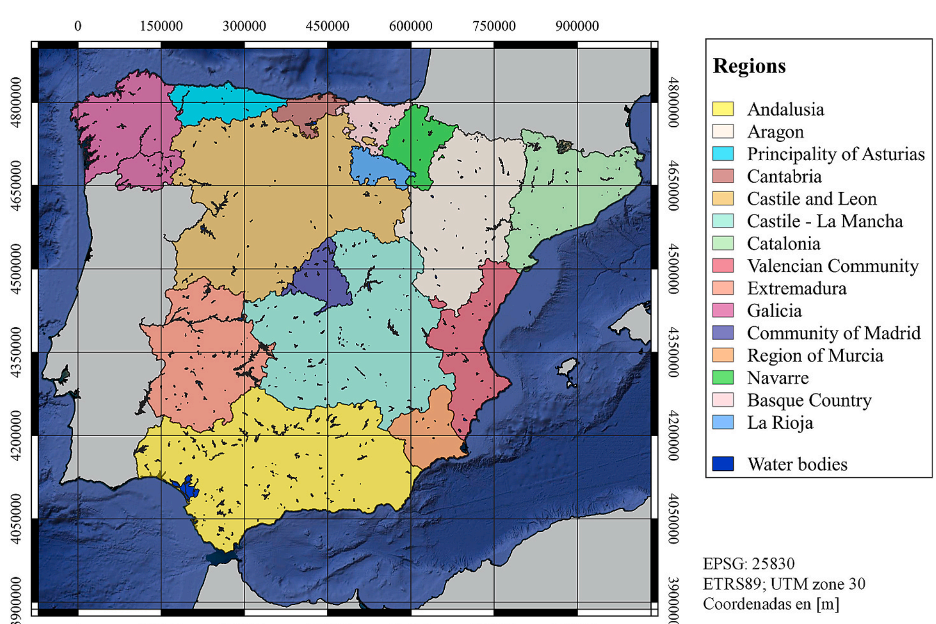

Fig. 2. Administrative regions in peninsular Spain.

Table 1
Data for bodies of water in peninsular regions of Spain and electricity generation (sources: MITECO (2019) and REE (2021)).

Region	Surface area [103·km^2]	# bodies of water	Water surface area [km^2]	Water bodies density [%]	Electricity demand in 2019 [TWh/year]	Electricity generation in 2019 [TWh/year]	Electricity generation from non-renewable energy in 2019 [% of total]
Andalusia	87.60	150	1563.46	1.78	39.82	34.01	37.9
Aragon	47.72	59	256.87	0.54	10.81	15.35	54.0
Asturias	10.60	12	11.71	0.11	9.41	10.12	33.2
Cantabria	5.32	5	63.43	1.19	4.19	2.30	18.1
Castile and Leon	94.22	78	400.75	0.43	14.21	22.40	85.2
Castile-La Mancha	79.46	112	471.20	0.59	12.14	22.85	53.0
Catalonia	31.11	113	92.34	0.30	46.95	45.21	16.1
Valencia	23.26	34	133.97	0.58	27.27	18.86	19.5
Extremadura	41.63	71	916.68	2.20	4.97	21.03	22.1
Galicia	29.58	47	160.79	0.54	18.40	24.85	65.2
Madrid	8.03	18	55.93	0.70	28.41	1.36	31.9
Murcia	11.31	8	14.69	0.13	9.46	10.47	18.0
Navarre	10.39	11	20.58	0.20	5.16	7.47	47.0
Basque Country	7.23	20	26.40	0.36	16.32	8.23	13.6
Rioja	5.05	7	5.44	0.11	1.70	2.58	49.3
TOTAL	492.52	745	4194.24	0.85	249.22	247.09	38.9

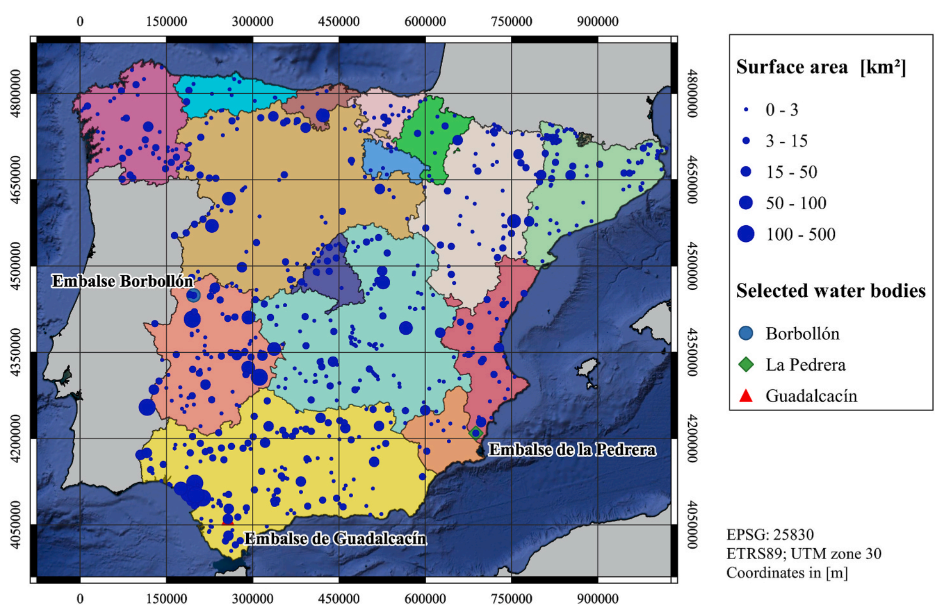

Fig. 3. Surface area of water bodies in peninsular Spain (source: MITECO (2019)).

Borbollón (Extremadura) (Fig. 3).

A review of the literature showed that different criteria have been applied to define the useful water surface area for FPV module deployment, a parameter that directly affects its electricity generation potential. According to Kim et al. (2019), a reservoir should have a minimum water depth over time for smooth installation and operation

Table 2
Water volume storage, water elevation, total surface area, useful surface area and FPV coverage for three dam reservoirs in Spain.

Reservoir	Scenario	Storage volume [10^6 m^3]	Elevation [m]	Total surface area [10^3 m^2]	Useful surface area [10^3 m^2]	FPV coverage [%]
Borbollón	1	85.76	21.52	9419.82	9419.82	100
	2	85.76	21.52	9419.82	941.98	10
	3	85.76	21.52	9419.82	8321.80	88
	4	7.04	8.00	2163.90	1592.50	74
La Pedrera	1	246.95	55.88	12,724.55	12,724.55	100
	2	246.95	55.88	12,724.55	1272.45	10
	3	246.95	55.88	12,724.55	11,978.57	94
	4	5.93	14.00	1070.16	829.42	78
Guadalcacín	1	682.51	61.50	33,280.90	33,280.90	100
	2	682.51	61.50	33,280.90	3328.09	10
	3	682.51	61.50	33,280.90	31,339.93	94
	4	121.50	30.00	10,541.14	9416.80	89

of FPV systems, which implies a reduction in the useful water surface. As in other previous studies, this analysis was based on a minimum water depth of 2 m (Spencer et al., 2019). However, as the water level of a reservoir changes due to variations in water flow and other factors, such as flood control and dam operation, the water surface available for deploying FPV systems varies over time. The influence of both these factors on reservoir coverage and the consequent impact on FPV potential is examined and discussed further below.

Four scenarios with different useful water surface areas were defined (Table 2). The reference scenario, or Scenario 1, was the total water surface coverage area reported by MITECO, which could then be used to estimate the full PFV potential. Scenario 2 considered only 10% cover, as in previous analyses in the literature. The third and fourth scenarios include the minimum water depth restriction. Thus, in Scenario 3, areas with water depths of less than 2 m were subtracted from the total water surface area provided by MITECO. In Scenario 4, the depth criterion was applied to the minimum water surface area in each reservoir over the past 20 years.

The characteristic area-elevation curves of the reservoirs (Fig. 4) were used to apply the depth reduction criterion to Scenarios 3 and 4. With these data, the water elevation of a given surface area can be determined and the minimum water depth is subtracted from it. Then, the useful water surface area can be found directly from the characteristic area-elevation curve.

The 1999–2020 water storage volume time series were used to define the minimum water surface area of each reservoir (Fig. 4). Once the minimum volume had been identified, the corresponding water surface area and water elevation were found with the characteristic area-volume and elevation-area curves, respectively. Then, the depth criteria reduction was applied to the water elevation, and the useful water surface area was found from the characteristic elevation-area curve.

Both the characteristic curves and water storage volume time series for each reservoir were provided by the corresponding Hydrographic Confederation, the regional water authority responsible for water catchment management under the MITECO.

2.4. FPV generation potential

2.4.1. General formula

The electricity generated by a FPV array over a given period of time was found by Marion (2010) as

$$E = \sum_{i=1}^{n} \eta_{PV} P_{STC} \left(\frac{G}{G_{STC}}\right) [1 - \alpha_P (T_C - T_{STC})] N \Delta t_i \quad (1)$$

where: η_{PV} is the individual PV module derating factor, which accounts for wiring losses, inverter inefficiency, component failures, soiling and aging, among other effects ($\eta_{PV} = 0.85$ here); P_{STC} is the nominal power of an individual PV module in terms of power output under Standard Test Conditions (STC); G is the effective, or plane-of-array irradiance, i.e. incident irradiance less self-shading losses; G_{STC} is the reference plane-of-array (POA) irradiance under STC = 1 kW/m^2; α_P is the PV panel temperature coefficient of power; T_C is the operating cell temperature; T_{STC} is the STC operating cell temperature = 25 °C; N is the number of installed PV modules; and Δt_i is the duration of the n time steps considered.

All these parameters present uncertainties that affect the FPV system performance. According to Thevenard and Pelland (2013), the combined uncertainty (standard deviation) for the average yield of a PV system is approximately 8.7% for the first year of operation, and 7.9% for the entire lifetime. Extending the present study to account for this uncertainty in FPV performance is left for future work, in which precise statistical distributions of variables with a particularly relevant impact on the performance of these systems should be addressed (e.g., T_c, which is affected by the water-cooling effect).

2.5. Global effective irradiance

G depends on the local solar irradiance, and its angle of incidence on the solar panel. Note that for a PV module with a horizontal or flat configuration and no self-shading, G is equal to the global horizontal irradiance (E_g). This parameter is found as described below.

The nominal POA irradiance (I) is the sum of the incident beam

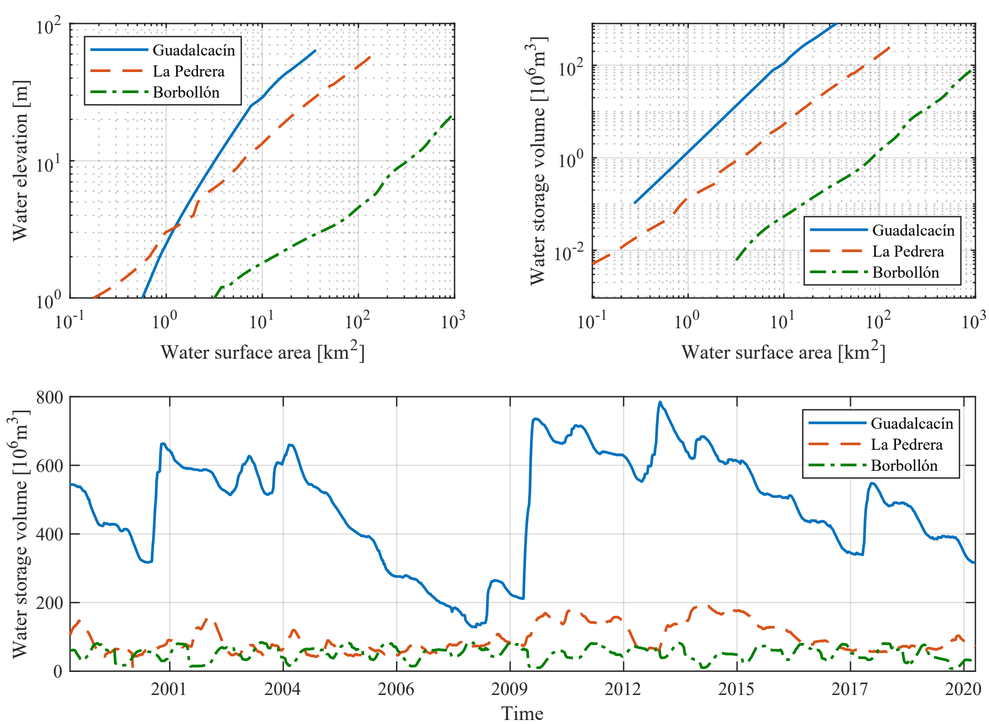

Fig. 4. Reservoir characteristic curves (upper panel) and water storage volumes (lower panel) for the three dam reservoirs.

irradiance, incident diffuse irradiance, and incident ground-reflected irradiance:

$$I = I_d + I_b + I_r \tag{2}$$

The incident diffuse irradiance (I_d) is solar energy that has been scattered by the atmosphere before reaching the surface of the FPV module. In this study, the computational method described by Perez et al. (1988) and Perez et al. (1990) was applied to find I_d, which accounts for both isotropic and circumsolar diffuse radiation, as well as horizon brightening. Incident beam irradiance (I_b) is solar energy that reaches the surface in a straight line from the sun:

$$I_b = E_b \cos(AOI) \tag{3}$$

where: E_b is the normal beam irradiance and AOI, the sun angle of incidence. The incident ground-reflected irradiance (I_r) is solar energy reflected from the ground that reaches the array surface and can be found as a function of the beam normal irradiance and solar zenith angle, sky diffuse irradiance, and albedo as follows (Liu and Jordan, 1963)

$$I_r = 0.5\rho(E_b \cos Z + E_d)(1 - \cos\beta) \tag{4}$$

where ρ is the ground reflectance (albedo).

Self-shading is shading of PV modules in one row of an array by modules in a neighbouring row. The sky diffuse, beam, and ground-reflected components of the effective irradiance after shading are:

$$G_d = I_d S_{dss} \tag{5}$$

$$G_b = I_b S_{bns} \tag{6}$$

$$G_r = I_r S_{rss} \tag{7}$$

where: S_{dss} is the sky diffuse factor, S_{bns} is the beam irradiance shading factor, and S_{rss} is the ground diffuse factor. If there is no self-shading, then $S_{dss} = S_{rss} = 1$. The algorithm proposed by Deline et al. (2013) was applied to calculate these three factors for each location and time step in Equation (1), which optimizes the separation between the PV panels in the array depending on their tilt angle. Once these factors and the effective components of irradiance have been found, global effective irradiance after shading is given by

$$G = G_d + G_b + G_r \tag{8}$$

2.6. Temperature correction

The operating cell temperature has a significant role in the performance assessment of any PV installation. The formula proposed by Kamuyu et al. (2018) accounts for the water-cooling effect and was used to obtain the operating cell temperature of FPV modules,

$$T_C = e_0 + e_1 T_a + e_2 G_T - e_3 V_w \tag{9}$$

where: T_a is the air temperature, V_w is the wind speed, and $e_0 = 2.0458$ °C, $e_1 = 0.9458$ °C^{-1}, $e_2 = 0.0215$ °C·m^2·day·kWh^{-1}, and $e_3 = 1.2376$ °C·s·m^{-1} are empirically determined coefficients.

2.7. Technical specifications of the FPV modules

FPV systems commonly installed on lakes and reservoirs consist of common PV modules over rigid pontoons that provide buoyancy to the system (Sujay et al., 2017). Nonetheless, flexible systems floating on the waterline have also been proposed to reduce loading on the structure and its mooring (Fig. 2) (Trapani and Millar, 2014). There are five main types of photovoltaic technologies: crystalline silicon, cadmium telluride and cadmium sulphide, organic and polymer cells, hybrid photovoltaic cells and thin film technology (Parida et al., 2011). Crystalline silicon is usually used for rigid pontoon systems (only available in a rigid format), whereas thin film systems have been proposed for flexible systems (Trapani et al., 2013). Rigid FPV systems with crystalline silicon modules (see technical specifications in Table 3), were used here as they are the predominant technology (Parida et al., 2011).

2.8. FPV performance indicators

Of the several parameters commonly used to assess the performance of renewable energy, the capacity factor, specific energy yield, GHG reduction and Levelized Cost of Energy (LCOE) were used here. The capacity factor of a FPV system (CF) is an important parameter that shows the ratio of the actual energy generated (E) over the maximum energy a system can generate (Zubair et al., 2020),

$$CF = \frac{E}{\sum_{i=1}^{n} P_{STC} N \Delta t_i} 100 \tag{10}$$

The specific energy yield of a FPV system is another relevant metric that can be found by dividing the energy delivered by the system over a given period of time by its footprint area, $SE = E/S$ (Rehman et al., 2007).

GHG reduction refers to the amount of GHG released by renewable energy power generation compared to the same amount of power generated by a fossil fuel energy system. It can be found by multiplying the emission reference value, which in Spain was 0.19 tCO_2eq/MWh in 2019 (REE, 2021), by the amount of FPV energy that can be generated.

Finally, the LCOE of FPV systems was found by dividing their entire lifecycle cost by their cumulative electricity generation. For this generic analysis, some simplifications were used, mainly that residual value or decommissioning costs, taxes, subsidies/incentives and interest during construction were not taken into account. The LCOE was found by dividing the entire lifecycle cost of the FPV systems by their cumulative electricity generation as follows (Kost et al., 2013),

$$\mathrm{LCOE} = \frac{I_0 + \sum_{t=1}^{n} \frac{A_t}{(1+r)^t}}{\sum_{t=1}^{n} \frac{E_t}{(1+r)^t}} \tag{11}$$

where: I_0 is the investment in construction and installation, also known as capital expediture (CAPEX); A_t is the total annual operating cost per year t in the FPV lifetime n ($t = 1, 2, \ldots, n$); r is the discount rate; and E_t is the electricity generated in the respective year as found with Eq. (1), which includes the FPV system degradation rate.

I_0 and A_t were based on a typical 50-MW FPV installation with a 20-year operating lifecycle. An $I_0 = 620$ €/kW was used for the CAPEX of large-scale FPV projects in 2018 (World Bank Group, 2019). A_t includes the inflation-adjusted costs related to operation and maintenance (O&M), insurance, and inverter warranty period. O&M costs were assumed to be 9.35 €/kW for the first year. Insurance is an optional cost that depends on the likelihood of extreme weather events and the percentage of the revenues insured. In this study, the total cost of insurance used was 0.3% of the total CAPEX, paid annually and adjusted for inflation (Speer et al., 2010). Like ground-mounted PV plants, some

Table 3
Technical specifications of the reference PV module.

Parameter	Value	Units
P_{STC}	375	W
Efficiency	19.3	%
α_P	−0.39	%°C^{-1}
Length	1.96	m
Width	0.99	m
Surface	1.95	m^2
Weight	26.0	kg
Material	Si monocrystalline	–
Manufacturer	Trina Solar	–

components of the floating plants require replacement during their operating lifetime. The inverters, which are assumed to be replaced about 1.33 times during the 20-year period, present the highest risk. The nominal amount of all inverter warranty expenses during operation was calculated on an annual basis of 3.4 €/kW (World Bank Group, 2019). The nominal discount rate for net present value calculations is defined based on the weighted average cost of capital (WACC), which varies depending on country and scenario. For Organisation for Economic Co-operation and Development (OECD) countries, which includes Spain, the WACC is $r = 7.5\%$ (IRENA, 2020).

2.9. Geospatial datasets

2.9.1. Solar irradiance

Solar radiation data is required for assessing the solar energy resource and estimating the performance of FPV systems. As shown in Eq. (1), Global Horizontal Irradiance (E_g) is the required parameter, which is commonly acquired from satellite-based datasets. In this study, the datasets from the Climate Monitoring Satellite Application Facility (CM-SAF) were used (Schulz et al., 2009). These data were retrieved from the Photovoltaic Geographical Information System (PVGIS), a web application widely used for estimating PV system performance in Europe (Huld et al., 2012). The main source of data for the CM-SAF radiation dataset is Meteosat geostationary satellite images, which cover an overall area from about 70°N to 70°S and from 70°W to 70°E. A previous validation of E_g using data from 20 ground stations has shown that the overall mean bias errors of this dataset is low, at about +2.0%, while the standard deviation of individual station mean bias errors is 5.0% (Amillo et al., 2014). (For methods used to calculate the solar radiation from satellite images see Amillo et al. (2014) and Mueller et al. (2012, 2009). Fig. 5 shows the average E_g in peninsular Spain, which varies from 147 to 235 W/m^2. As expected from their lower latitude, irradiance is higher in the southern than in the northern regions. A slight variation in this parameter is also observed between western (Atlantic) and eastern regions (Mediterranean).

2.10. Wind speed and air temperature

According to Equation (12), the cell temperature of a PV module varies depending on the atmospheric conditions and, in particular, wind speed, V_w, and air temperature, T_a. Time series of these parameters for the period 2012–2016 were obtained for each body of water in Fig. 3 from the data available in the Copernicus Atmosphere Monitoring Service (CAMS), which provides the European Centre for Medium-Range Weather Forecasts (ECMWF) latest global reanalysis dataset (ERA5) (Inness et al., 2019). The time series of V_w were obtained by combining the eastward and northward components of the “neutral wind” at a height of 10 m above the surface of the Earth, whereas T_a time series were directly acquired from the ECMWF. Uncertainty characterisation of these variables is not provided by CAMS. However, information regarding the bias for specific variables and diverse spatial and temporal domains can be found in Hersbach et al. (2020). For example, a global fit of the analysis to observations of T_a, revealed that the monthly-mean analysis fit varies between 0 and −0.16 °C. Molina et al. (2021) compared wind speed observations from 245 stations across Europe with ERA5 corresponding reanalysis values and concluded that the data from the reanalysis is “valuable information to perform further detailed studies with a regular spatial and time wind distribution, from the climatological or renewable energy perspectives”.

The average T_a and V_w in continental Spain are shown in Fig. 6 and Fig. 7, respectively. In general, and again as expected from their lower latitude, the average air temperature is higher in southern than in northern regions. Average wind speeds are highest in the coastal regions, particularly those in the northwest.

3. Results and discussion

3.1. FPV energy potential

The annual FPV electricity generation was estimated for each water body in peninsular Spain using Eq. (1) and taking into account the global horizontal irradiance and the water-cooling effect at each site. A flat PV module configuration, which maximizes the electricity generation per surface area, and a typical 10% coverage of the water surface area were assumed (Scenario 3). Fig. 8 maps the results of this analysis.

Under the above assumptions, FPV systems in Spanish continental water bodies could produce nearly 80 TWh of electricity per year, which represents about 31% of the country’s total electricity demand and 15.2·10^6 tCO_2 equivalent GHG emissions (Table 1, Table 4). If the full FPV potential of the country were harnessed, the electricity generation from non-renewable energy could be reduced by 81% and GHG emissions by 6%, contributing to meet the EU 55% reduction target for 2030.

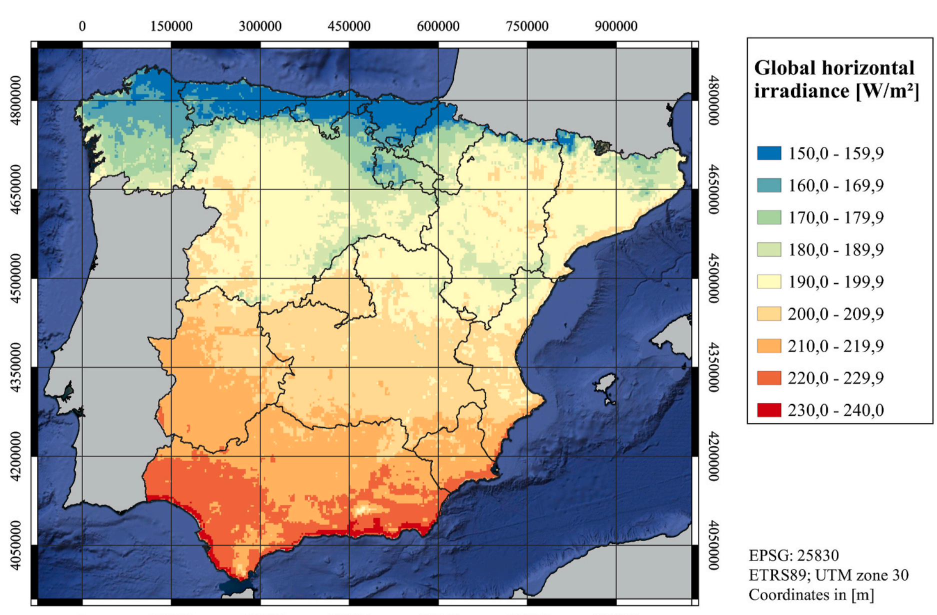

Fig. 5. Average global horizontal irradiance (E_g) in peninsular Spain.

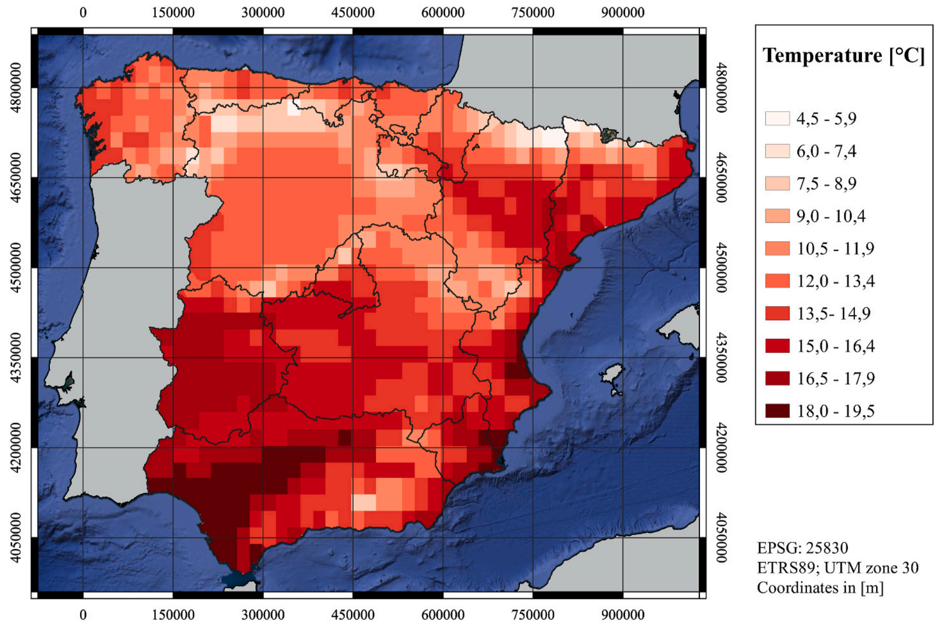

Fig. 6. Average air temperatures (T_a).

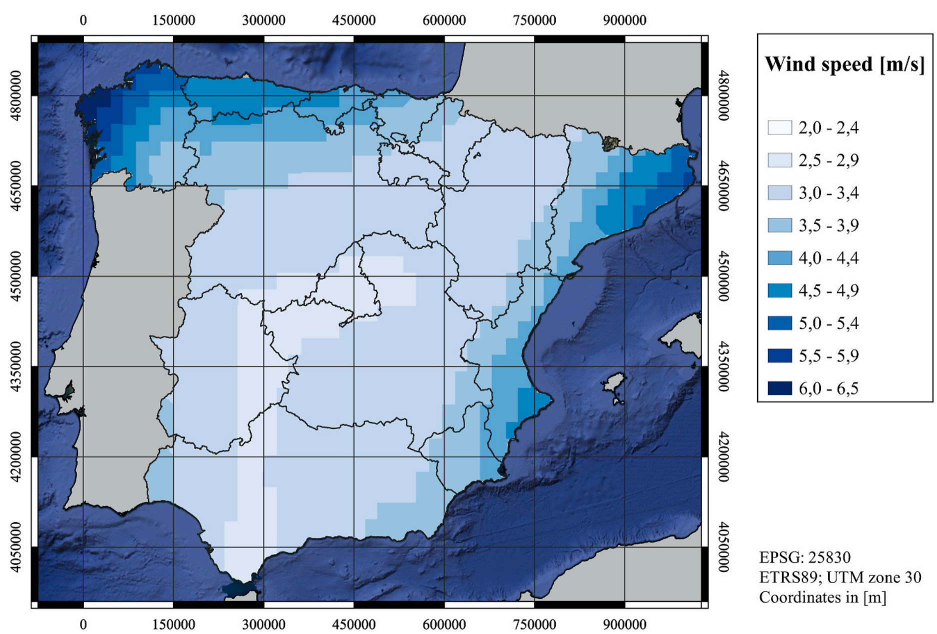

Fig. 7. Average wind speed (V_{10}).

Nevertheless, as similar FPV potential assessments in other countries have applied higher coverage of water bodies, these results may underestimate the true potential of floating solar energy in Spain.

Of the total FPV potential, 55.94 TWh/year of electricity would be generated in highly modified or artificial water bodies (mainly dam reservoirs), and the rest in natural water bodies. If FPV systems are installed only in the former, 22% of the country's electricity demand could be supplied with this renewable energy. In this case, the reduction in electricity generated from non-renewables would drop from 81 to 58%. However, this result is subject to variations in reservoir water surface and the FPV water depth restriction as discussed in the following section.

The highest production is found in two natural bodies of water, the Doñana Wetlands, and the Doñana Lagoons, with 7.02 and 3.13 GWh/year, which also have the largest areas (Table 5). Both bodies are in the Doñana National Park, a natural reserve in Andalusia, where the installation of FPV systems could be restricted. They are followed by two dam reservoirs in Extremadura: The Alqueva Reservoir and the La Serena Reservoir, with 2.78 and 2.50 GWh/year, respectively.

Fig. 8 shows apparent regional differences in the FPV potential. The southern regions, especially Andalusia and Extremadura, show the highest generation potential. These two regions alone have over 60% of the country's total potential, and both could replace their non-renewable electricity generation with floating solar energy (Table 4) due to the large water area and abundant solar resource available in both regions (Figs. 3 and 5, respectively). In fact, Extremadura has three times more FPV generation potential than its electricity demand.

On the contrary, some regions have a residual FPV electricity generation potential. The potential of Asturias, Catalonia, Madrid, Murcia, and the Basque Country is below 5% of their electricity demand. The

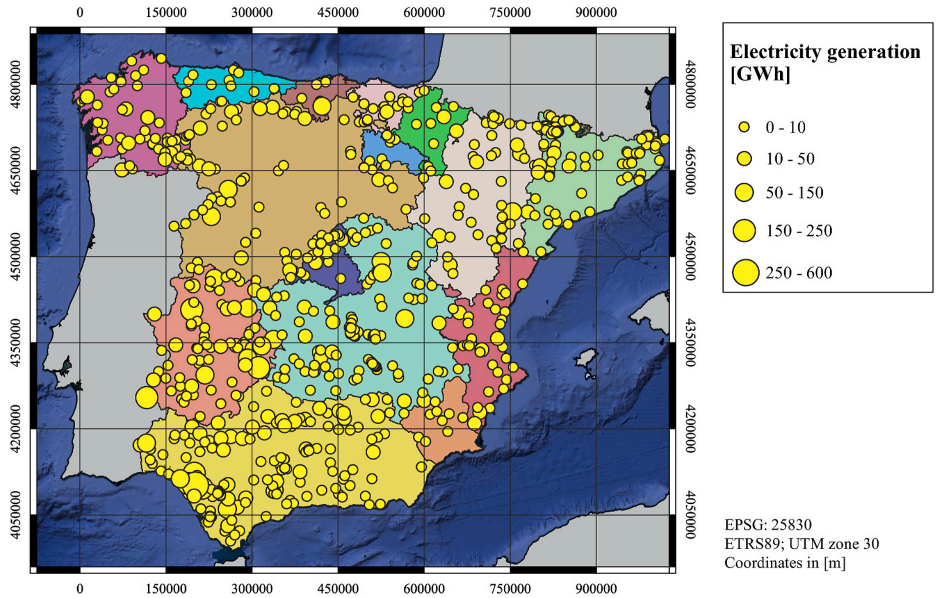

Fig. 8. Potential annual energy produced with FPV systems at each continental water body in Spain.

Table 4
Estimated electricity generation potential with FPV systems and actual electricity generation potential with ground-mounted PV systems in peninsular regions of Spain (source: [1]).

Region	Estimated FPV potential[a]		Actual ground-mounted PV potential	
	Electricity generation [TWh/year]	CF [%]	Electricity generation [TWh/year]	CF [%]
Andalusia	31.21	18.58	3.47	14.70
Aragon	4.56	16.53	1.51	15.63
Asturias	0.17	13.56	0.00	5.77
Cantabria	0.99	14.51	0.00	12.31
Castile and Leon	6.95	16.58	1.11	14.98
Castile-La Mancha	8.44	16.83	3.08	18.12
Catalonia	1.61	16.24	0.38	15.45
Valencia	2.46	17.09	0.53	16.49
Extremadura	17.13	21.97	2.39	10.61
Galicia	2.61	15.13	0.02	13.57
Madrid	1.02	16.98	0.08	14.84
Murcia	0.27	17.32	1.85	16.62
Navarre	0.33	15.00	0.28	19.42
Basque Country	0.39	13.64	0.06	14.04
Rioja	0.09	14.78	0.14	16.47
TOTAL	78.24	18.26	14.91	14.84

[a] applying 10% coverage of the water surface area.

Table 5
Top 10 bodies of water in FPV generation potential in peninsulaar Spain.

Water body	Natural (N) or highly modified/artificial (H/A)	UTM coordinates [km]		Total surface area [km^2]	FPV electricity generation, E[a] [TWh/year]
		x	y		
Doñana Wetlands	N	201	4102	345.77	7.02
Doñana Lagoons	N	189	4104	152.24	3.13
Alqueva Reservoir (Principal)	H/A	137	4300	144.78	2.78
La Serena Reservoir	H/A	311	4306	137.07	2.50
Coto del Rey Lagoons	H/A	199	4122	105.14	2.11
Veta de la Palma	H/A	213	4096	103.08	2.09
Alcántara II Reservoir	H/A	195	4407	100.92	1.92
Abalario Lagoons	N	175	4113	81.25	1.68
Buendía Reservoir	H/A	527	4471	84.33	1.50
Almendra Reservoir	H/A	229	4570	84.53	1.47

[a] covering 10% of the total water surface area.

results for Madrid are the consequence of its high electricity demand and small area (28.41 TWh per year in only 8030 km^2). The result for Asturias, Catalonia, Murcia, and Basque Country is explained by their low water body density (Table 1).

Other regions with intermediate FPV generation potential could significantly reduce their dependence on non-renewable energy and/or balance their electricity supply and demand by installing FPV solar plants in continental water bodies. Cantabria, for example, could cover its current non-renewable electricity generation, 18% of its total electricity generation, by deploying its full FPV potential.

Bearing in mind the novelty of FPV technology and the scarcity of projects, the validation of the FPV electricity generation potential in bodies of water in Spain with actual data could not be addressed. Nonetheless, the obtained FPV estimates were compared with the actual performance of ground-mounted PV solar farms in terms of CF (Eq. (10)). The values estimated for the FPV technology are consistent with the actual values for ground-mounted solar farms in most of the regions, with a difference of only 3.4% in the total CF of Spain (Table 4). In general, the values of CF are higher for FPV systems, which is explained by their improved performance due to the water-cooling effect.

3.2. Detailed water body selection analysis

The section above gave a preliminary analysis of electricity generation in Spanish water bodies assuming a conservative scenario of 10% water surface coverage and PV modules with a horizontal configuration. In this section, the potential electricity generation of FPVs is reanalysed for a selection of three specific dam reservoirs, the Borbollón, La Pedrera and Guadalcacín (Fig. 9). Calculations made for four reservoir coverage

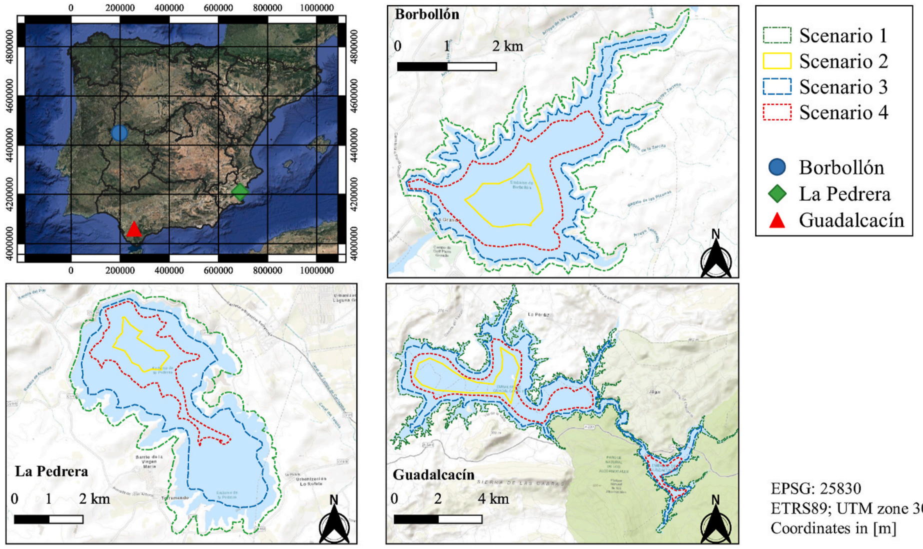

Fig. 9. Dam reservoirs analysed with water surface contours of each FPV coverage scenario.

scenarios (Table 2) and five PV module tilt angles (0, 10, 20, 30 and 40°) are presented and performance indicators found are discussed.

The highest electricity generation was found for a horizontal PV module configuration in Scenario 1, which is the full PFV potential (Fig. 10). The Guadalcacín shows the highest potential for all scenarios and tilt angles, with a maximum $E = 7.1$ GWh per year. The differences in the potential electricity generation between the four scenarios in each reservoir are apparent. Scenario 1 has the highest potential, as it considers the total water surface area useful (Table 2). It is followed by Scenario 3, which applies the FPV system deployment depth restriction to the total water surface area, with electricity generation 5–12% lower than under Scenario 1, depending on the reservoir.

A comparison of the results under Scenarios 2 and 4 shows that the one with the highest FPV electricity generation potential depends on the reservoir. According to Equation (1), the reason for this is the differences in the useful water surface area (Table 2). While the Borbollón and Guadalcacín have the highest potential under Scenario 4, the opposite holds for La Pedrera. In fact, the latter has a higher FPV potential than the Borbollón under all scenarios except Scenario 4 (Fig. 10). It should be recalled that under Scenario 2, coverage is 10% (typical coverage in the literature used in the section above), while the depth restriction under Scenario 4 is the minimum historic water surface area at each reservoir. This result highlights the need to consider seasonal variations in the water storage volume of dam reservoirs in detailed assessments of their FPV generation potential rather than a fixed coverage.

The FPV maximum specific energy yield potential is achieved with flat PV modules (Fig. 11). The highest is at the Guadalcacín with $SE = 212.8$ GWh/km^2, followed by the La Pedrera with $SE = 210.6$ GWh/km^2 and the Borbollón with $SE = 199.3$ GWh/km^2. The *SE* decreases with PV module tilt angle by about 51% from 0° to 40° at these reservoirs.

The capacity factor also varies with the PV module tilt angle (Fig. 11). The highest CF is found with a 10° tilt angle, where $CF =$ 12.69, 12.55 and 11.88% at the Guadalcacín, La Pedrera and Borbollón reservoirs, respectively. These results suggest that FPV module configurations other than horizontal may be of greater interest in terms of power production investment. Nonetheless, the results of the *CF* for the different tilt angles are still very similar, as the separation between PV modules is optimized to reduce self-shading (Section 2.4.2). Note that both *SE* and *CF* are independent of reservoir coverage, i.e., the *CF* and *SE* for a given reservoir are equivalent under the different scenarios.

The LCOE for the three reservoirs and different PV module tilt angles as presented in Fig. 11, range from 74.89 €/MWh at the Guadalcacín with a 10° tilt angle to 80.50 €/MWh at the Borbollón with a 40° tilt angle. This falls within the range found in literature for this type of energy conversion technology. As expected from the *CF* presented in the section above, the lowest LCOE is found with a 10° tilt angle at all reservoirs.

4. Conclusions

This study presented, for the first time, the potential of FPV systems for electricity generation in bodies of freshwater in continental Spain. A preliminary assessment included natural, highly modified, and artificial bodies of water and assumed a conservative 10% coverage of their surface area. The regional and national FPV potential for electricity generation was evaluated, and the results were compared with the current electricity demand and non-renewable electricity generation. As artificial bodies of water may be better suited for the deployment of floating solar energy systems, three dam reservoirs were then analysed in detail. Variations in the water level over time and FPV operation depth restrictions were included in the analysis to reduce uncertainty in reservoir coverage, which directly affects estimates of the electricity generation potential, by defining four different scenarios for each body of water. Several conclusions about the FPV energy potential in Spain and some recommendations for future research in this field are discussed below.

By covering 10% of the continental water surface in Spain with horizontal FPV modules, roughly 80 TWh per year, or 31% of the country's electricity demand, could be generated. Moreover, floating solar energy systems could contribute to an 81% reduction in electricity generated from non-renewable energy resources and 6% GHG. Although the FPV generation potential falls to 56 TWh per year if natural bodies of water are excluded, it would still represent a substantial 22% of the country's electricity demand and 51% of the non-renewable electricity generated.

Apart from reducing their dependence on non-renewable energy, Spanish regions could benefit from FPV energy by balancing their electricity generation and demand. Southern regions and Andalusia and Extremadura would especially benefit, as they have large water surface areas and high solar irradiance levels. The sum of the FPV electricity generation potential of these two regions alone is over 60% of the country's total potential and could supply its entire electricity demand.

Nonetheless, these general results have several uncertainties and/or limitations. First, some natural bodies of water may not be open to deployment of FPV systems, especially in those in environmentally sensitive areas, such as Doñana National Park, where the two bodies of

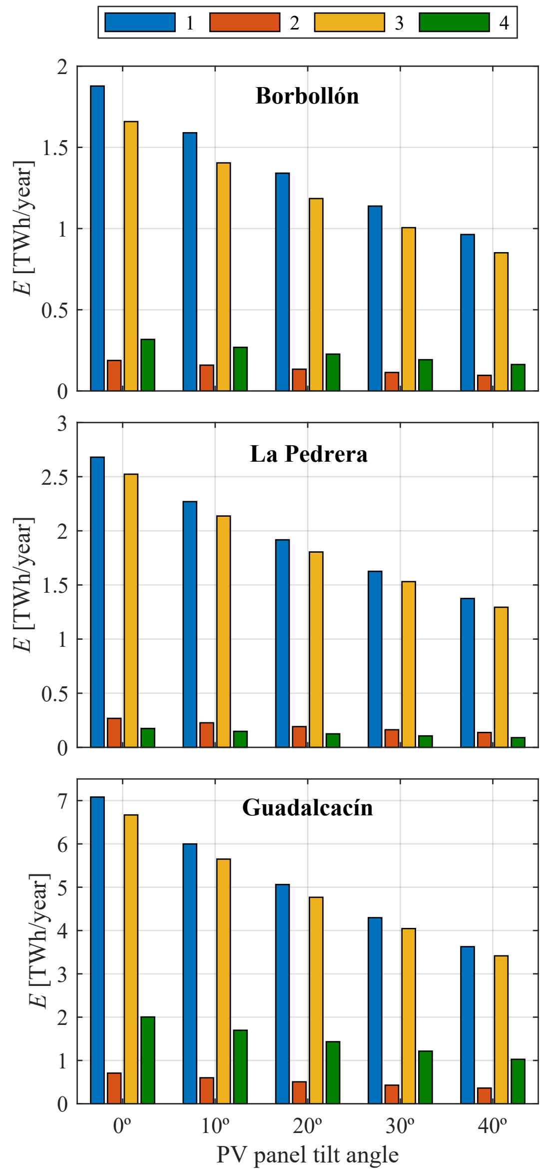

Fig. 10. FPV electricity generation potential for the Borbollón, La Pedrera and Guadalcacín reservoirs under four reservoir coverage scenarios at five PV module tilt angles.

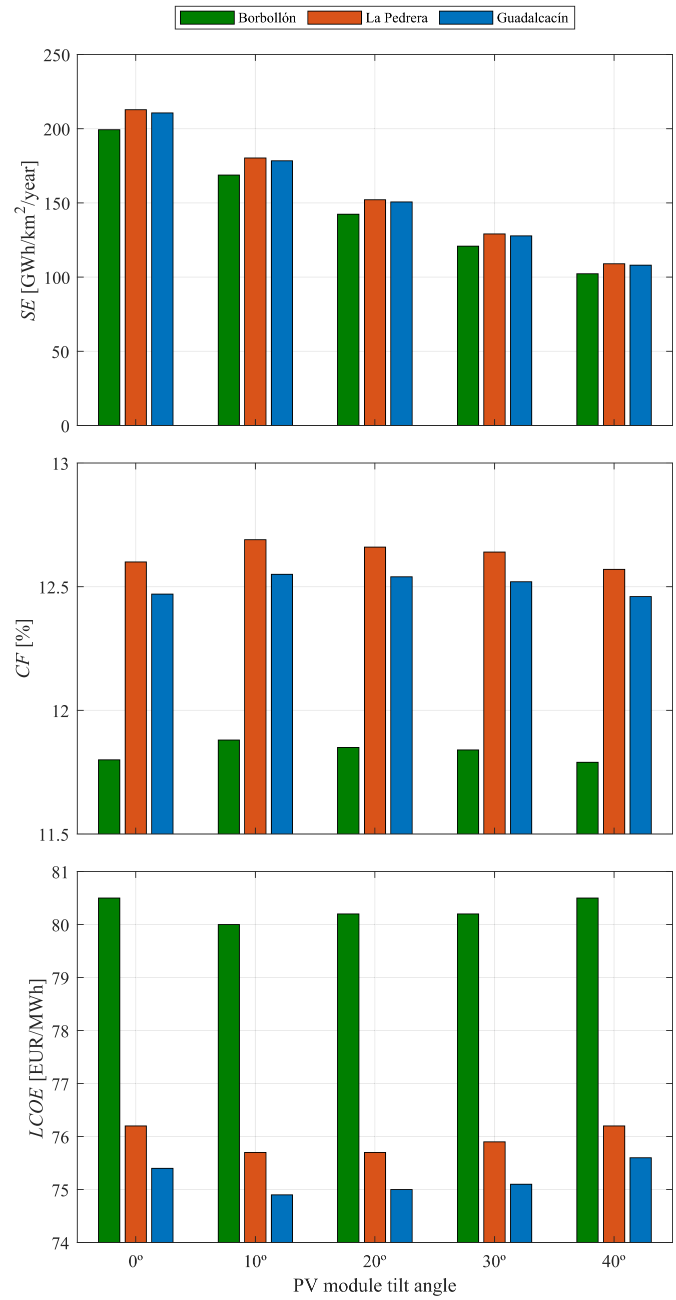

Fig. 11. Specific energy yield (*SE*), Capacity Factor (*CF*) and Levelized Cost of Energy (LCOE) for the Borbollón, La Pedrera and Guadalcacín reservoirs at five different PV module tilt angles.

water with the highest electricity generation potential are located. Second, a low 10% water surface coverage was assumed, and third, bodies of water with a small area are not included in available datasets. Therefore, the estimates of the FPV generation potential presented here may be conservative.

Although this and previous studies have commonly applied a fixed percentage of coverage to assess the FPV potential on national or regional scale, this approach may not be adequate for a precise assessment. The analysis of three dam reservoirs showed that assuming a fixed percentage for this parameter may result in misleading calculations of the true FPV electricity generation potential. Both variations in the water elevation (especially in dam reservoirs, which are subjected to both seasonal and operational variations of the water storage volume) and FPV operational depth restrictions should be applied for precise estimation of the FPV electricity generation potential of a body of water. Therefore, the reservoir's characteristic curves and history of water levels, which are not always available, are required to define the actual useful water surface area.

Summarizing, FPV is a real renewable energy alternative that can help Spain to implement the 2030 55% GHG emissions reduction target. Some regions and particularly those in the south could benefit greatly from harnessing this renewable energy, not only by reducing their dependence on non-renewable resources, but also by balancing their electricity mix. Finally, further research is required to improve future assessments of the FPV electricity generation potential, for example by comparing the resulting estimates with the amount measured from actual FPV panels and performing a detailed sensitivity analysis.

CRediT authorship contribution statement

M. López: Conceptualization, Methodology, Software, Formal analysis, Investigation, Resources, Writing – original draft, Writing – review & editing, Supervision, Project administration, Funding acquisition. **F. Soto:** Software, Formal analysis, Investigation, Investigation, Resources, Writing – review & editing, Visualization. **Z.A. Hernández:** Conceptualization, Methodology, Investigation, Resources, Writing – review & editing, Funding acquisition.

Declaration of competing interest

The authors declare that they have no known competing financial interests or personal relationships that could have appeared to influence the work reported in this paper.

Acknowledgments

This work was partially supported by the City Council of Gijón through the Instituto Universitario de Tecnología Industrial de Asturias [University Institute of Industrial Technology of Asturias] (IUTA) (Ref. SV-19-GIJON-1-10). The views and opinions expressed herein do not necessarily reflect those of the IUTA.

References

Amillo, A.G., Huld, T., Müller, R., 2014. A new database of global and direct solar radiation using the eastern meteosat satellite, models and validation. Rem. Sens. 6, 8165–8189. https://doi.org/10.3390/rs6098165.

Cazzaniga, R., Cicu, M., Rosa-Clot, M., Rosa-Clot, P., Tina, G.M., Ventura, C., 2017. Compressed air energy storage integrated with floating photovoltaic plant. J. Energy Storage 13, 48–57. https://doi.org/10.1016/j.est.2017.06.006.

Deline, C., Dobos, A., Janzou, S., Meydbray, J., Donovan, M., 2013. A simplified model of uniform shading in large photovoltaic arrays. Sol. Energy 96, 274–282. https://doi.org/10.1016/j.solener.2013.07.008.

El Hammoumi, A., Chalh, A., Allouhi, A., Motahhir, S., El Ghzizal, A., Derouich, A., 2021. Design and construction of a test bench to investigate the potential of floating PV systems. J. Clean. Prod. 278, 123917. https://doi.org/10.1016/j.jclepro.2020.123917.

World Bank Group, Esmap, S.E.R.I.S., 2019. Where Sun Meets Water: Floating Solar Handbook for Practitioners.

European Comission, 2000. *Directive 2000/60/EC of the European Parliament and of the Council of 23 October 2000 establishing a framework for Community action in the field of water policy*. Office for Official Publications of the European Communities.

Feldman, D., Barbose, G., Margolis, R., Wiser, R., Darghouth, N., Goodrich, A., 2015. In: Photovoltaic (PV) Pricing Trends: Historical, Recent, and Near-Term Projections. https://doi.org/10.2172/1172243.

Girard, A., Gago, E.J., Ordoñez, J., Muneer, T., 2016. Spain's energy outlook: a review of PV potential and energy export. Renew. Energy 86, 703–715. https://doi.org/10.1016/j.renene.2015.08.074.

Gomez-Exposito, A., Arcos-Vargas, A., Gutierrez-Garcia, F., 2020. On the potential contribution of rooftop PV to a sustainable electricity mix: the case of Spain. Renew. Sustain. Energy Rev. 132, 110074. https://doi.org/10.1016/j.rser.2020.110074.

Gonzalez Sanchez, R., Kougias, I., Moner-Girona, M., Fahl, F., Jäger-Waldau, A., 2021. Assessment of floating solar photovoltaics potential in existing hydropower reservoirs in Africa. Renew. Energy 169, 687–699. https://doi.org/10.1016/j.renene.2021.01.041.

Gorjian, S., Sharon, H., Ebadi, H., Kant, K., Scavo, F.B., Tina, G.M., 2021. Recent technical advancements, economics and environmental impacts of floating photovoltaic solar energy conversion systems. J. Clean. Prod. https://doi.org/10.1016/j.jclepro.2020.124285.

Hersbach, H., Bell, B., Berrisford, P., Hirahara, S., Horányi, A., Muñoz-Sabater, J., Nicolas, J., Peubey, C., Radu, R., Schepers, D., Simmons, A., Soci, C., Abdalla, S., Abellan, X., Balsamo, G., Bechtold, P., Biavati, G., Bidlot, J., Bonavita, M., De Chiara, G., Dahlgren, P., Dee, D., Diamantakis, M., Dragani, R., Flemming, J., Forbes, R., Fuentes, M., Geer, A., Haimberger, L., Healy, S., Hogan, R.J., Hólm, E., Janisková, M., Keeley, S., Laloyaux, P., Lopez, P., Lupu, C., Radnoti, G., de Rosnay, P., Rozum, I., Vamborg, F., Villaume, S., Thépaut, J.N., 2020. The ERA5 global reanalysis. Q. J. R. Meteorol. Soc. 146, 1999–2049. https://doi.org/10.1002/qj.3803.

Huld, T., Müller, R., Gambardella, A., 2012. A new solar radiation database for estimating PV performance in Europe and Africa. Sol. Energy 86, 1803–1815. https://doi.org/10.1016/j.solener.2012.03.006.

Inness, A., Ades, M., Agustí-Panareda, A., Barré, J., Benedictow, A., Blechschmidt, A.-M., Dominguez, J.J., Engelen, R., Eskes, H., Flemming, J., Huijnen, V., Jones, L., Kipling, Z., Massart, S., Parrington, M., Peuch, V.-H., Razinger, M., Remy, S., Schulz, M., Suttie, M., 2019. The CAMS reanalysis of atmospheric composition. Atmos. Chem. Phys. 19, 3515–3556. https://doi.org/10.5194/acp-19-3515-2019.

Irena, I., 2020. Renewable Power Generation Costs in 2019. Report. Int. Renew. Energy Agency, Abu Dhabi.

Kamuyu, W.C.L., Lim, J.R., Won, C.S., Ahn, H.K., 2018. Prediction model of photovoltaic module temperature for power performance of floating PVs. Energies 11. https://doi.org/10.3390/en11020447.

Kim, S.-M., Oh, M., Park, H.-D., 2019. Analysis and prioritization of the floating photovoltaic system potential for reservoirs in Korea. Appl. Sci. 9, 395. https://doi.org/10.3390/app9030395.

Kost, C., Mayer, J.N., Thomsen, J., Hartmann, N., Senkpiel, C., Philipps, S.P., Nold, S., Lude, S., Saad, N., Schmid, J., 2013. Levelized Cost of Electricity: PV and CPV in comparison to other technologies. others Fraunhofer Ise.

Liu, B.Y.H., Jordan, R.C., 1963. The long-term average performance of flat-plate solar-energy collectors. With design data for the U.S., its outlying possessions and Canada. Sol. Energy 7, 53–74. https://doi.org/10.1016/0038-092x(63)90006-9.

Liu, L., Sun, Q., Li, H., Yin, H., Ren, X., Wennersten, R., 2019. Evaluating the benefits of integrating floating photovoltaic and pumped storage power system. Energy Convers. Manag. 194, 173–185. https://doi.org/10.1016/j.enconman.2019.04.071.

López, M., Rodríguez, N., Iglesias, G., 2020. Combined floating offshore wind and solar PV. J. Mar. Sci. Eng. 8 https://doi.org/10.3390/JMSE8080576.

Marion, W.F., 2010. Overview of the PV Module Model in PVWatts. National Renewable Energy Laboratory.

Martín-Martínez, S., Cañas-Carretón, M., Honrubia-Escribano, A., Gómez-Lázaro, E., 2019. Performance evaluation of large solar photovoltaic power plants in Spain. Energy Convers. Manag. 183, 515–528. https://doi.org/10.1016/j.enconman.2018.12.116.

Merida García, A., Gallagher, J., Crespo Chacón, M., Mc Nabola, A., 2021. The environmental and economic benefits of a hybrid hydropower energy recovery and solar energy system (PAT-PV), under varying energy demands in the agricultural sector. J. Clean. Prod. 303, 127078. https://doi.org/10.1016/j.jclepro.2021.127078.

MITECO, 2019. Ministerio para la Transición Ecológica [WWW Document]. Masas agua PHC (2015-2021), Minist. para la Transic. Ecológica. URL. https://www.miteco.gob.es/es/cartografia-y-sig/ide/descargas/agua/masas-de-agua-phc-2015-2021.aspx, 2.1.21.

Molina, M.O., Gutiérrez, C., Sánchez, E., 2021. Comparison of ERA5 surface wind speed climatologies over Europe with observations from the HadISD dataset. Int. J. Climatol. 41, 4864–4878. https://doi.org/10.1002/joc.7103.

Mueller, R.W., Matsoukas, C., Gratzki, A., Behr, H.D., Hollmann, R., 2009. The CM-SAF operational scheme for the satellite based retrieval of solar surface irradiance - a LUT based eigenvector hybrid approach. Remote Sens. Environ. 113, 1012–1024. https://doi.org/10.1016/j.rse.2009.01.012.

Mueller, R., Behrendt, T., Hammer, A., Kemper, A., 2012. A new algorithm for the satellite-based retrieval of solar surface irradiance in spectral bands. Rem. Sens. 4, 622–647. https://doi.org/10.3390/rs4030622.

Oliveira-Pinto, S., Stokkermans, J., 2020. Assessment of the potential of different floating solar technologies – Overview and analysis of different case studies. Energy Convers. Manag. 211, 112747. https://doi.org/10.1016/j.enconman.2020.112747.

Oliveira-Pinto, S., Rosa-Santos, P., Taveira-Pinto, F., 2020. Assessment of the potential of combining wave and solar energy resources to power supply worldwide offshore oil and gas platforms. Energy Convers. Manag. 223, 113299. https://doi.org/10.1016/j.enconman.2020.113299.

Padilha Campos Lopes, M., de Andrade Neto, S., Alves Castelo Branco, D., Vasconcelos de Freitas, M.A., da Silva Fidelis, N., 2020. Water-energy nexus: floating photovoltaic systems promoting water security and energy generation in the semiarid region of Brazil. J. Clean. Prod. 273, 122010. https://doi.org/10.1016/j.jclepro.2020.122010.

Parida, B., Iniyan, S.S., Goic, R., 2011. A review of solar photovoltaic technologies. Renew. Sustain. Energy Rev. 15, 1625–1636. https://doi.org/10.1016/J.RSER.2010.11.032.

Perez, R., Stewart, R., Seals, R., Guertin, T., 1988. The development and verification of the Perez diffuse radiation model. Sandia Rep.

Perez, R., Ineichen, P., Seals, R., Michalsky, J., Stewart, R., 1990. Modeling daylight availability and irradiance components from direct and global irradiance. Sol. Energy 44, 271–289. https://doi.org/10.1016/0038-092X(90)90055-H.

Pimentel Da Silva, G.D., Branco, D.A.C., 2018. Is floating photovoltaic better than conventional photovoltaic? Assessing environmental impacts. Impact Assess. Proj. Apprais. 36, 390–400. https://doi.org/10.1080/14615517.2018.1477498.

Pringle, A.M., Handler, R.M., Pearce, J.M., 2017. Aquavoltaics: synergies for dual use of water area for solar photovoltaic electricity generation and aquaculture. Renew. Sustain. Energy Rev. 80, 572–584. https://doi.org/10.1016/j.rser.2017.05.191.

Ranjbaran, P., Yousefi, H., Gharehpetian, G.B., Astaraei, F.R., 2019. A review on floating photovoltaic (FPV)power generation units. Renew. Sustain. Energy Rev. 110, 332–347. https://doi.org/10.1016/j.rser.2019.05.015.

Redón Santafé, M., Torregrosa Soler, J.B., Sánchez Romero, F.J., Ferrer Gisbert, P.S., Ferrán Gozálvez, J.J., Ferrer Gisbert, C.M., 2014. Theoretical and experimental analysis of a floating photovoltaic cover for water irrigation reservoirs. Energy 67, 246–255.

REE, 2021. REData: statistical data [WWW Document] REData statical data, Red Eléctrica Española (REE). URL. https://www.ree.es/es/datos/aldia, 2.1.21.

Rehman, S., Bader, M.A., Al-Moallem, S.A., 2007. Cost of solar energy generated using PV panels. Renew. Sustain. Energy Rev. 11, 1843–1857. https://doi.org/10.1016/j.rser.2006.03.005.

Santafé, M.R., Ferrer Gisbert, P.S., Sánchez Romero, F.J., Torregrosa Soler, J.B., Ferrán Gozálvez, J.J., Ferrer Gisbert, C.M., 2014. Implementation of a photovoltaic floating cover for irrigation reservoirs. J. Clean. Prod. 66, 568–570. https://doi.org/10.1016/j.jclepro.2013.11.006.

Schulz, J., Albert, P., Behr, H.D., Caprion, D., Deneke, H., Dewitte, S., Dürr, B., Fuchs, P., Gratzki, A., Hechler, P., Hollmann, R., Johnston, S., Karlsson, K.G., Manninen, T., Müller, R., Reuter, M., Riihelä, A., Roebeling, R., Selbach, N., Tetzlaff, A., Thomas, W., Werscheck, M., Wolters, E., Zelenka, A., 2009. Operational climate monitoring from space: the EUMETSAT satellite application facility on climate monitoring (CM-SAF). Atmos. Chem. Phys. 9, 1687–1709. https://doi.org/10.5194/acp-9-1687-2009.

Skoplaki, E., Palyvos, J.A., 2009. On the temperature dependence of photovoltaic module electrical performance: a review of efficiency/power correlations. Sol. Energy 83, 614–624. https://doi.org/10.1016/j.solener.2008.10.008.

Song, J., Choi, Y., 2016. Analysis of the potential for use of floating photovoltaic systems on mine pit lakes: case study at the Ssangyong open-pit limestone mine in Korea. Energies 9, 1–13. https://doi.org/10.3390/en9020102.

Speer, Bethany, Mendelsohn, Michael, Cory, Karlynn, 2010. Insuring Solar Photovoltaics: Challenges and Possible Solutions.

Spencer, R.S., Macknick, J., Aznar, A., Warren, A., Reese, M.O., 2019. Floating photovoltaic systems: assessing the technical potential of photovoltaic systems on man-made water bodies in the continental United States. Environ. Sci. Technol. 53, 1680–1689. https://doi.org/10.1021/acs.est.8b04735.

Sujay, P.S., W, M.M., N, S.N., S, P.D.S., Wagh, M.M., Shinde, N.N., Patil, S.S., Wagh, M. M., Shinde, N.N., 2017. A review on floating solar photovoltaic power plants. Int. J. Sci. Eng. Res. 8, 789–794.

Taboada, M.E., Cáceres, L., Graber, T.A., Galleguillos, H.R., Cabeza, L.F., Rojas, R., 2017. Solar water heating system and photovoltaic floating cover to reduce evaporation: experimental results and modeling. Renew. Energy 105, 601–615. https://doi.org/10.1016/j.renene.2016.12.094.

Thevenard, D., Pelland, S., 2013. Estimating the uncertainty in long-term photovoltaic yield predictions. Sol. Energy 91, 432–445. https://doi.org/10.1016/j.solener.2011.05.006.

Tina, G.M., Cazzaniga, R., Rosa-Clot, M., Rosa-Clot, P., 2018. Geographic and technical floating photovoltaic potential. Therm. Sci. 22, 831–841. https://doi.org/10.2298/TSCI170929017T.

Trapani, K., Millar, D.L., 2013. Proposing offshore photovoltaic (PV) technology to the energy mix of the Maltese islands. Energy Convers. Manag. 67, 18–26. https://doi.org/10.1016/j.enconman.2012.10.022.

Trapani, K., Millar, D.L., 2014. The thin film flexible floating PV (T3F-PV) array: the concept and development of the prototype. Renew. Energy 71, 43–50. https://doi.org/10.1016/J.RENENE.2014.05.007.

Trapani, K., Millar, D.L., Smith, H.C.M., 2013. Novel offshore application of photovoltaics in comparison to conventional marine renewable energy technologies. Renew. Energy 50, 879–888. https://doi.org/10.1016/j.renene.2012.08.043.

Zubair, M., Bilal Awan, A., Ghuffar, S., Butt, A.D., Farhan, M., 2020. Analysis and selection criteria of lakes and dams of Pakistan for floating photovoltaic capabilities. J. Sol. Energy Eng. 142, 1–11. https://doi.org/10.1115/1.4045352.